34th Annual International Conference of the IEEE EMBS
San Diego, California USA, 28 August - 1 September, 2012

Estimation of Excitatory Drive from Sparse Motoneuron Sampling

Yao Li, *Member, IEEE*, Lauren H. Smith, Levi J. Hargrove *Member, IEEE*,
Douglas J. Weber, *Member, IEEE*, and Gerald E. Loeb, *Senior Member, IEEE*

Abstract— **It is possible to replace amputated limbs with mechatronic prostheses, but their operation requires the user's intentions to be detected and converted into control signals sent to the actuators. Fortunately, the motoneurons (MNs) that controlled the amputated muscles remain intact and capable of generating electrical signals, but these signals are difficult to record. Even the latest microelectrode array technologies and targeted motor reinnervation (TMR) can provide only sparse sampling of the hundreds of motor units that comprise the motor pool for each muscle. Simple rectification and integration of such records is likely to produce noisy and delayed estimates of the actual intentions of the user. We have developed a novel algorithm for optimal estimation of motor pool excitation based on the recruitment and firing rates of a small number (2-10) of discriminated motor units. We first derived the motor estimation algorithm from normal patterns of modulated MN activity based on a previously published model of individual MN recruitment and asynchronous frequency modulation. The algorithm was then validated on a target motor reinnervation subject using intramuscular fine-wire recordings to obtain single motor units.**

I. Introduction

When humans perform a motor task, the central nervous system (CNS) excites the alpha motoneurons (MNs) to activate the muscles, which in turn actuate the skeletal segments to perform the task. For amputees, the motor pathway - from supraspinal structures to spinal cord to peripheral nerve - remains intact and capable of generating and transmitting electrical signals. The activity of surviving MNs can be recorded from the ventral horn, ventral roots [1] or peripheral nerves [2] to infer the prosthesis user's intentions and to control the prosthetic actuators (Fig.1), but only if the signals enable a rapid and accurate estimate of the excitatory drive to the whole pool of MNs.

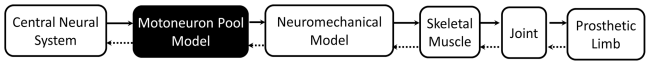

Fig.1. Stages of neural signal transmission for human motor control system.

Even with the state-of-the-art microelectrode array technologies, only a few of the hundreds of MUs supplying each of the many amputated muscles (the MN pool, MNP) are likely to be recorded. A given ventral root or peripheral nerve trunk normally innervates on the order of 10-20 functionally distinct muscles. Obtaining 100 channels of data from ventral root nerve or TMR muscle is challenging and the average yield rate of discriminable units tends to be less than one unit per channel. This means any single MNP will be represented by ~5 MUs on average but with a large stochastic range.

In an early study from Hoffer et al [1, 3], a total of 150 fine flexible wire microelectrodes were implanted chronically in the fifth lumbar ventral root of 17 cats during locomotion on a treadmill. These microelectrodes yielded records of the natural discharge patterns of 164 individual axons, where only 51 axons were identified as MNs projecting to the anterior thigh muscle group. Similarly, targeted motor reinnervation results in patchy innervations [4, 5]. EMG signals recorded transcutaneously or intramuscularly are likely to consist of small numbers of discriminable single MUs [6] whose amplitude may not accurately reflect their relative MN size or recruitment order.

The amplitudes of the action potentials recorded from each MU depend on the vagaries of electrode location with respect to the current source of the MU (whether that source is the motor axon or the patch of muscle fibers that has been reinnervated) rather than the size or recruitment order of the MU itself. Simply rectifying and integrating the electrical signals of MUs, as is done with gross EMG from intact muscles [7], may not produce an accurate estimate of MNP excitation. Thus, the challenge is to develop an algorithm that can make the best possible estimate of MNP excitation from the recruitment and firing rates of a small number (2-10) of discriminable MUs.

II. Algorithm Design

The firing frequency of early recruited MUs correlates well with onset of the simultaneously recorded EMG signals from the whole muscle in animals, which, in turn, reflects the excitation of the whole MNP. The later recruited MUs generally start firing when the excitation reaches a specific threshold level. Their frequency is then modulated according to the time course of the excitation amplitude above this threshold, which can be measured from the EMG signals [1].

We used these properties to design a novel estimation scheme for the MNP activation over the entire range of recruitment. The algorithm is called *Sparse Optimal Motor Estimation* (SOME). It works by mapping the instantaneous firing rate of each recorded MU into the excitation level that tends to cause that MU activity. The SOME algorithm predicts a total excitation level for the MNP, which can be fed into a model of the limb to estimate actual muscle force output and the resulting kinematics.

Yao Li and Gerald Loeb are with the Department of Biomedical Engineering, University of Southern California, Los Angeles, CA USA 90089 (Phone: +213-821-1114, Email: Yao.Li.1@usc.edu, gloeb@usc.edu).

Douglas J. Weber is with the Department of Physical Medicine and Rehabilitation, University of Pittsburgh, Pittsburgh, PA USA 15260 (Phone: +412-624-4055, Email: djw50@pitt.edu).

Levi Hargrove and Lauren Smith are with the Center for Bionic Medicine at the Rehabilitation Institute of Chicago and the Department of Physical Medicine and Rehabilitation, Northwestern University, Chicago, IL, USA, 60611 (Phone: +312-238-2084, Email: l-hargrove@northwestern.edu).

A. *Sparse Sampling of MNP*

We first set the parameters for a MNP recruitment model with *N* discriminable MUs. The relationship between the net excitatory drive u and firing rate for each MU_i was defined as $f_i(u)$, $i = 0, 1, 2, ...N$. The MNP recruitment model is fully defined when all *N* MUs are available and the dimensionality of the MN set is N. The challenging problem is how to reconstruct the net excitatory drive u from a sparse sampling of the entire MNP, which has a much smaller number of discriminable MUs than N. A simple saturating recruitment model is utilized, in which the slow MU starts to fire at 5imp/s when excitation reaches 10mV, and the firing rate saturates at the 20imp/s when the excitation input is 25mV and above. The fast MU starts to fire at 10imp/s when excitation reaches 20mV and plateaus at a peak firing rate of 40imp/s when the excitation exceeds 30mV. The firing rate ranges are based on the default values in Virtual Muscle [8], which normalizes firing rates according to $f_{0.5}$, the firing frequency that produces half the maximal tetanic force for each MU (10 imp/s for slow MU, 20 imp/s for fast MU).

In the example provided here, the sparse MNP model has only two MUs: MU_1 (the first recruited slow unit) and MU_2 (the last recruited fast unit). For each motor unit MU_i, $r_i^k = 1/(s_i^k - s_i^{k-1})$ is the instantaneous firing rate of k^{th} spike at the spike timing s_i^k. It is also a function of the excitation input at the sampled spike timing, which is defined as $r_i^k = f_i[u(s_i^k)]$., and their firing rates over the full range of net excitatory drive to the MNP were simulated according to the relationship shown in Figure 2.

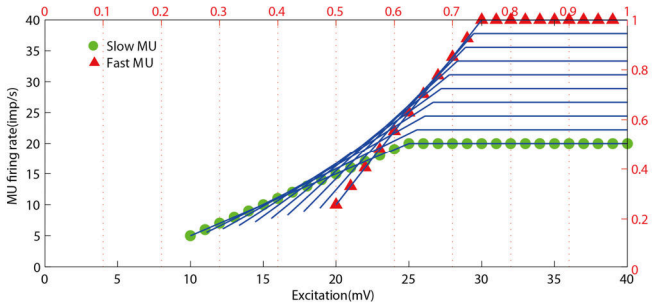

Fig 2. Simulated firing relationship of two MUs in a saturating MNP.

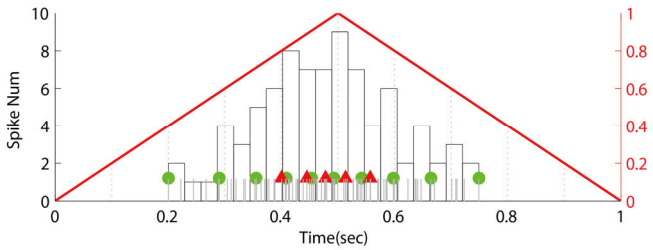

Fig3. The spikes of two MUs of the entire motor neuron pool

A simple triangular ramp was used as the excitation input approximating similar physiological experiments [9, 10] and simulated spike occurrences for the two MUs are depicted in Figure 3. The histogram distribution (unfilled bar) is plotted for the spike timing with bin size of 50ms under the normalized excitation input (scale on the right). The aggregate activity of the asynchronous units is very noisy, even when integrated into 50ms bins typical for updating command signals to prosthetic systems.

B. *Sparse Optimal Motor Estimation Algorithm*

The frequent occurrence of individual MU spikes provides an opportunity to implement much more frequent and less noisy estimates of MNP excitation, which is exploited by the SOME algorithm:

Sparse Optimal Motor Estimation Algorithm

Input: Spike timing vector of observed MUAPs
$\underline{s} = [\ t_0 \quad t_1 \quad \cdots \quad t_j \quad \cdots \quad t_m\ ]$
Input: Calibrated function $f_i(u)$ for observed MU_i
Output: Estimated excitation input $\hat{u}(t)$

1 **START**
2 $\hat{u}(t) = 0$ for $t = [0, t_0)$
3 $\hat{u}(t_0) = \mathbf{min}\{\epsilon_i, \forall\, i\}$
3 **WHILE** $|\underline{s}| \neq 0$
4 **IF** $f_i[\hat{u}(t_{j-1})] \leq 1/(t_j - t_{j-1}),\ \exists\, i$
5 $u(s_i^k) = \mathbf{max}\left\{f_i^{-1}[1/(t_j - t_{j-1})], \forall\, i\right\}$
6 $\hat{u}(t) = u(s_i^k)$ for $t = [t_{j-1}, t_j]$
7 $j = j++$
8 **IF** $f_i[\hat{u}(t_{j-1})] > 1/(t_j - t_{j-1}),\ \forall\, i$
9 $\hat{u}(t) = u(s_i^{k-1})$ for $t = [t_{j-1}, t_{j-1} + 1/r_i^{k-1})$
10 $\hat{u}(t) = u(s_i^{k-1}) * e^{-\gamma(t - t_{j-1} - 1/r_i^{k-1})}$ for $t = [t_{j-1} + 1/r_i^{k-1}, t_j]$
11 $j = j++$
12 **END WHILE**
13 **END**

SOME algorithm employs different strategies for rising ramp and falling ramp. After determining the rising trend (line 4-7), when the firing rate for a given MU at the previous estimate of excitation level is less than or equal to the current instantaneous spike rate, the estimation can only be updated on the occurrence of each successive MU spike, so estimate tends to lag behind the actual MNP excitation. In the falling trend scenario (line 8-11), when a spike is expected given the previous excitation level and the time elapsed since the last spike for all MUs, the absence of a spike that is "due" to occur given the previous interval can be used to estimate the maximal level of excitation that is consistent with the absence of spikes. If no spikes occur in any MUs, then the excitation estimate falls rapidly from one exponential to another according to the lowest trajectory and updates as exponential decay (line 10) where γ is the decreasing rate that could be arbitrarily set between 0 and 1.

The output of the *SOME* algorithm is illustrated by the gray solid trace in Figure 4. For comparison, the true excitatory input is plotted in red ramp trace and the actual spike occurrences are labeled by dots and triangle with sequential number). As excitation increases ($0 \leq t \leq 0.5$ i), the first spike (#1) and subsequent spikes (#2-9) timing provides successively higher and momentarily accurate estimates of the total excitation drive. As excitation decreases ($0.5 \leq t \leq 1$), the estimates start to drop as individual spikes that were "due" to occur (e.g., spike #14) given the previous (e.g., spike #13) estimate fail to occur. The interval between individual

motor unit action potential (MUAP) is fairly long (100 to 200ms for 10 to 5imp/s, respectively) compared to the rate at which the excitation signal to the MNP may actually be modulated. Waiting for the next spike in a given train or aggregating the asynchronous events and taking a running average tends to be slow and/or noisy; therefore it is imperative to derive as much information as possible from the timing of each spike in MUAP trains.

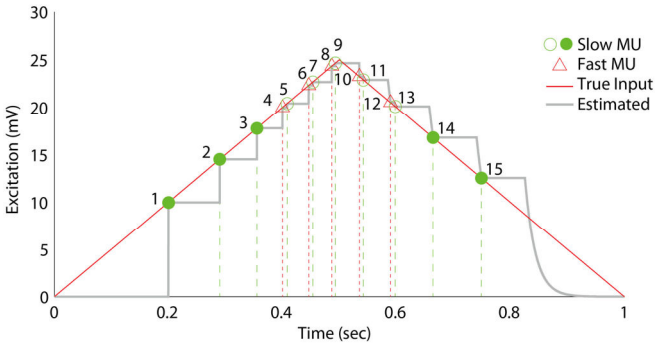

Fig 4. Estimated excitation input (gray solid line) based on the MUAPs from the slow MU (dot) and fast MU (triangle) using proposed SOME algorithm

III. Validation with Experimental Data

In order to use the SOME algorithm with an amputee, it is necessary to calibrate the threshold and frequency modulation of each available MU in terms of the intended excitation to each MNP. In validation experiments using intact human or animal subjects, the gross EMG from the parent muscle is available for calibration, but no such signal is available from an amputee. Instead, it will be crucial to instruct subjects to perform a set of virtual movements with systematic ramping of effort to associate the MU activity with a particular muscle function. In the case of muscles operating on multiple degrees of freedom in the skeletal system, the imputed membership in a MNP will have to be extracted based on statistical correlations with multiple virtual movements that would normally require different combinations of muscle activation, which remain to be developed. In this experiment, a shoulder disarticulated amputee with TMR surgery was tracking a "virtual ramp of effort" of elbow extension by matching the integrated and smoothed surface EMG (sEMG) to a slowly rising visual ramp up to what the subject perceived was his/her maximal voluntary contraction (MVC).

The intramuscular EMG (iEMG) signals were recorded from bipolar fine wire electrodes (CareFusion) using a 10-channel Motion Lab Systems MA300 system with x4000 gain and sampled at 10 kHz by a National Instruments USB-6218 DAQ. The signal was bandpass filtered between 10Hz and 2KHz. Both the sEMG and iEMG signals were rectified, filtered and normalized to the MVC level. Two MU firing patterns were discriminated from the iEMG signal according to their distinctive waveforms (Fig. 5) during a voluntary ramp up to MVC. Their instantaneous firing rates were calibrated to excitatory drive as estimated from the smoothed sEMG (Fig. 6). The *SOME* algorithm was used to estimate MNP excitation during the ramp effort (red trace in Fig.7), which has been smoothed over 50ms bins for comparison with the similarly smoothed sEMG (light gray trace) and iEMG (dark gray trace).

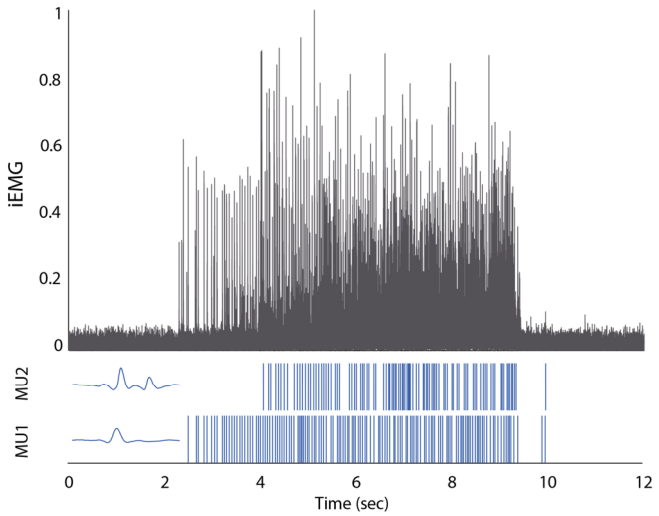

Fig 5. Extracted spike time and motor unit waveforms (20ms duration inserts) from the intramuscular EMG signal (top) during ramp effort.

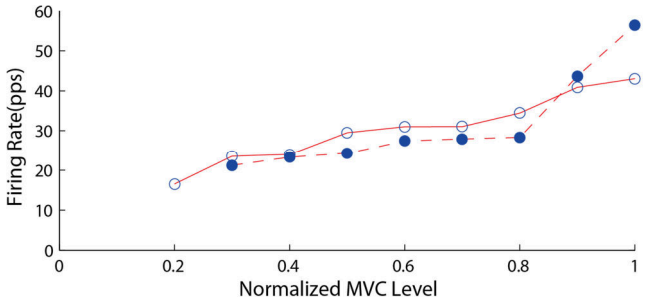

Fig 6. The instantaneous firing rates of the two MUs as a function of normalized sEMG amplitude from Fig. 5.

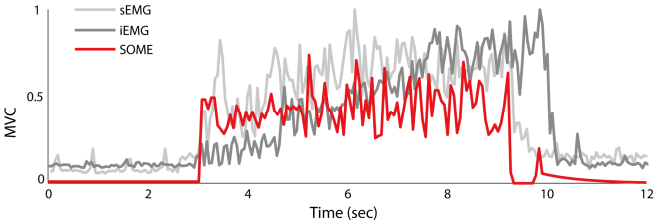

Fig 7. Comparison of SOME algorithm output (red trace) to sEMG (light gray trace) and iEMG (dark gray trace).

IV. Discussion and Conclusion

The validation experiment serves only to demonstrate the functionality of the SOME algorithm. It remains to be tested using novel data sets from those used to calibrate the MU firing rates. Such tests would preferably include more rapid fluctuations of effort, which would take advantage of the algorithm's ability to estimate excitation without the delays inherent in smoothing functions.

The use of the SOME algorithm assumes that there are no false positives or false negatives in the MU spike discrimination. The incidence of such errors will vary greatly with the method and quality of the recordings. A missed spike in a single MU train will result in an instantaneous drop of the

perceived rate. Such an error would be rapidly corrected if other MUs were contributing but could result in a substantial underestimate if only the one MU was active. Extra spikes such as misclassification of another MU can result in unphysiologically high perceived firing rates, which will need to be capped by other refinements to the algorithm. Because actual muscle recruitment tends to change smoothly during voluntary activity such as controlling prosthesis, a *Kalman* filter could probably be used to improve performance, but that is outside the scope of this study.

The sample record available from the TMR patient suggests that the SOME algorithm may be more suitable for ventral root and peripheral nerve recordings, where the unit waveforms tend to be much briefer and there is less background activity [1]. The relatively long and complex unit signatures obtained from these TMR muscles (e.g. MU2 in Fig. 5) may be a feature of the reinnervation process and will make it particularly difficult to obtain suitable spike discrimination when multiple units are active because of their tendency to overlap and occlude each other.

In the recordings available here from a slow ramp, there was relatively little difference between the rectified and smoothed sEMG and iEMG, so the SOME algorithm would not have provided any advantage. The SOME output had a somewhat different time course from the smoothed EMGs that may actually reflect the stepwise force generation typical of subjects following a target ramp with only visual feedback. There is no reason to believe that the EMG generated by the highly unusual motor unit distributions following TMR are an appropriate "gold standard" for the effort of the user. Whether SOME output is more accurate and useful for control will not be known until the two types of signal processing are compared in a complete control loop with a prosthesis capable of rapid responses to commands.

Studies have been done on sEMG signal to extract the firing of different motor units together with their recruitment time [12][13]. A linear relationship between MU firing rates and rectified and smoothed iEMG from the same normal muscle has been demonstrated experimentally before [14]. It tends to be a common initial firing frequency for MUs of a given type, and their firing frequencies converge to a single maximal firing frequency at maximal activation. There is a suggestion that the frequency modulation of earlier recruited units is hyperbolic rather than linear [15]. In order to use the SOME algorithm with an amputee, it is necessary to calibrate the threshold and frequency modulation of each available MU terms of the intended excitation to each MNP. In validation experiments using intact human or animal subjects, the gross EMG from the parent muscle is available for calibration, but no such signal is available from an amputee. Instead, it will be crucial to instruct subjects to perform a set of virtual movements with systematic ramping of effort to associate the MU activity with a particular muscle function. In the case of muscles operating on multiple degrees of freedom in the skeletal system, the imputed membership in a MNP will have to be extracted based on statistical correlations with multiple virtual movements that would normally require different combinations of muscle activation, which remain to be developed.

ACKNOWLEDGEMENT

This research is funded by DARPA/SPAWAR, Contract No. N66001-11-C4141, titled: Reliable Spinal Nerve Interfaces for Sensorimotor Neuroprotheses. Lauren H. Smith is supported by the Howard Hughes Medical Institute Medical Research Fellows Program.

REFERENCES

[1] Hoffer, J. A., Sugano, N., Loeb, G. E., Marks, W. B., O'Donovan, M. J., and Pratt, C. A., "Cat hindlimb motoneurons during locomotion. II. Normal activity patterns,"J.Neurophysiol., vol. 57, pp. 530-553, 1987.

[2] Branner, A., Stein, R. B., Fernandez, E., Aoyagi, Y., and Normann, R. A., "Long-term stimulation and recording with a penetrating microelectrode array in cat sciatic nerve," IEEE Transactions on Biomedical Engineering, vol. 51, pp. 146-157, 2004.

[3] Hoffer, J. A., O'Donovan, M. J., Pratt, C. A., and Loeb, G. E., "Discharge patterns in hindlimb motoneurons during normal cat locomotion," Science, vol. 213, pp. 466-468, 1981.

[4] Kuiken, T. A., Dumanian, G. A., Lipschutz, R. D., Miller, L. A., and Stubblefield, K. A., "The use of targeted muscle reinnervation for improved myoelectric prosthesis control in a bilateral shoulder disarticulation amputee,"Prosthet.Orthot.Int.,vl.28, pp.245-253, 2004

[5] Lowery, M. M., Weir, R. F., and Kuiken, T. A., "Simulation of intramuscular EMG signals detected using implantable myoelectric sensors (IMES)," IEEE Transactions on Biomedical Engineering, vol. 53, pp. 1926-1933, 2006.

[6] Borg, J., Grimby, L., and Hannerz, J., "Axonal conduction velocity and voluntary discharge properties of individual short toe extensor motor units in man," The Journal of Physiology, vol. 277, pp. 143-152, 1978.

[7] Loeb, G. E. and Gans, C., Electromyography for experimentalists. Chicago: University Chicago Press, 1986, pp. 38

[8] Cheng, E., Brown, I. E., and Loeb, G. E., "Virtual Muscle: A computational approach to understanding the effects of muscle properties on motor control," J.Neurosce.Methods, vol. 101, pp. 117-130, 2000.

[9] Kato, M., Murakami, S., and Yasuda, K., "Behavior of single motor units of human tibialis anterior muscle during voluntary shortening contraction under constant load torque," Experimental Neurology, vol. 90, pp. 238-253, 1985.

[10] Bawa, P., Chalmers, G. R., Jones, K. E., Søgaard, K., and Walsh, M. L., "Control of the wrist joint in humans," European Journal of Applied Physiology, vol. 83, pp. 116-127, 2000.

[11] Hauschild, M., Davoodi, R., and Loeb, G. E., "A virtual reality environment for designing and fitting neural prosthetic limbs," IEEE Trans Neural Syst.Rehabil Eng, vol. 15, pp. 1-7, 2007.

[12] Roberto Merletti, Aleš Holobar, Dario Farina, "Analysis of motor units with high-density surface electromyography", Journal of Electromyography and Kinesiology, Volume 18, Issue 6, Pages 879 - 890, December 2008.

[13] Aleš Holobar, Dario Farina, Marco Gazzoni, Roberto Merletti, Damjan Zazula, "Estimating motor unit discharge patterns from high-density surface electromyogram", Clinical Neurophysiology, Volume 120, Issue 3 , Pages 551-562, March 2009.

[14] Milner-Brown, H. S., Stein, R. B., and Yemm, R., "The orderly recruitment of human motor units during voluntary isometric contractions," Journal of Physiology, vol. 230, pp. 359-370, 1973.

[15] Monster, A. W. and Chan, H., "Isometric force production by motor units of extensor digitorum communis muscle in man," Journal of Neurophysiology, vol. 40, pp. 1432-1443, 1977.